Analysis of the Relative Stability of *cis*-Urocanic Acid in Condensed Phase. The Use of Langevin Dipoles

Jose Manuel Hermida-Ramón,[†] Gunnar Karlström,*[,†] and Roland Lindh[‡]

Department of Theoretical Chemistry and Department of Chemical Physics, Chemical Center, University of Lund, P.O.B. 124, S-221 00 Lund, Sweden

Received: April 8, 2002; In Final Form: May 20, 2002

A series of ab initio calculations employing a modified Langevin dipoles method to model neutral, cationic, and anionic *cis*-urocanic acid in human skin is presented. A comparison between the stability of the conformers in gas phase and in a condensed phase is performed. In particular, the energy barrier and transition state of the isomerization reaction of the anionic forms of *cis*-urocanic acid have been characterized. The modifications of the Langevin dipoles method, a procedure to obtain the required model parameters, and model verifications are presented. The latter include computing the water solvation energy and the free energy of the water dissociation.

1. Introduction

The role of the solvent can be crucial for the properties and reactivity of a substance in a condensed phase. The relative stability of different conformations of a substance and different transition states for a reacting molecule may change drastically because of the influence of the environment. Urocanic acid (UCA, (*E*)-3-(I′*H*-imidazol-4′-yl) propenoic acid) is an excellent example of this. The existence of an intramolecular hydrogen bond (IMHB) in *cis*-UCA has been shown by experimental[1−3] and theoretical methods.[4,5] The atoms taking part in this IMHB can rearrange via a proton-transfer reaction allowing for two different conformations for the neutral (see Figure 1,conformers **A** and **B**) and anionic (see Figure 1, conformers **D** and **E**) UCA. The stability of the different structures depends strongly on the characteristics of the environment. This makes the UCA molecule and anion interesting model systems in which the effect of the solvation due to the surrounding can be studied. However, a study of the UCA system is also significant because of the biophysiological importance of the system.[6,7] *trans*-UCA constitutes 0.7% of the weight in the uppermost layer of the human epidermis. Absorption of UV light in the skin induces the isomerization of *trans*-UCA to the cis isomer. *cis*-UCA alters immune responses in the body, resulting in systemic immune suppression,[8,9] which has importance in the carcinogenesis of skin malignancies and in the etiology of certain allergic illnesses of the skin. Furthermore, *cis*-UCA is also regarded as a good model to understand the behavior of many bioorganic molecules[10−12] because of its hydrogen bonds, which are analogous to what appears in proteins and nucleic acids.

The stability of the different neutral, cationic, and anionic conformations of UCA have been characterized in gas phase.[4,5] We could not find in the literature, however, any study of the relative stability of the different conformers of this substance in a condensed phase with properties similar to that present in the human skin. The present study will fill this gap by performing several ab initio calculations on the different structures of UCA. The environment is represented in these calculations by a set of dipoles and polarizabilities distributed on the lattice sites of a primitive cubic lattice. The coupling between the lattice dipoles and the molecular system will be treated in the mean field approximation.[13] This means in practice that the dipoles will be modeled using the Langevin dipoles model (LDM).[14−16] Technically, the used solvation model is similar to that developed by Warshel and co-workers.[15−18] There are, however, a few differences, and they will be described in detail in this work.

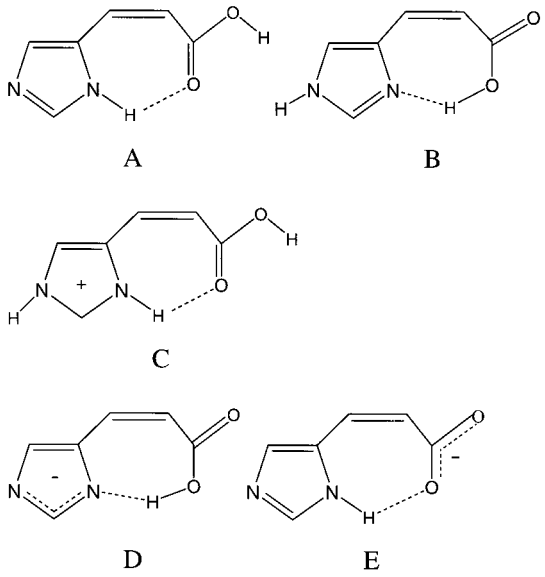

Figure 1. Geometries of the neutral (**A**, **B**), cationic (**C**), and anionic (**D**, **E**) *cis*-UCA conformations.

The next two sections describe briefly the LDM and the procedure followed for its parametrization. Technical details on the calculations will also be described in these sections. In the following section, the results are presented and discussed.

2. Method and Computational Details

In this section, we will describe the procedure used to model the effect of the environment on the UCA molecule. The use

[†] Department of Theoretical Chemistry.
[‡] Department of Chemical Physics.

10.1021/jp025893r CCC: $22.00
Published on Web 06/19/2002

of LDM for this purpose is not new, and it has already been used by several groups.[15,18−22] Alternatively, the so-called polarized continuum model (PCM) could have been used.[23] The main drawbacks of that approach is that it only takes into account for the particle nature of a medium by the effective size of the cavity and that it does not model effects of dielectric saturation. The starting point for our implementation of the LDM is a primitive cubic lattice. In each lattice point, a dipole and a polarizability is located.[18,24] Here, we can note the first deviation in this work from the most standard type of lattice models, which have *either* a dipole *or* a polarizability in each lattice point. We have chosen to have *both* a dipole and a polarizability. The dipole should model the rotational degrees of freedom for the molecules described by the lattice, and the polarizabilities are introduced to describe the electronic degrees of freedom. The contribution to the response from vibrational motion is presently ignored. The studied molecular system is then located in the lattice, and lattice points that are close to the target molecule are modified by its presence (for details see below).

As is clear from the presentation above, the description of the lattice requires three parameters. These are the shortest distance between two lattice sites and the polarizability and the dipole moment of a lattice site. As was mentioned above, the response of a dipole to the field on the dipole is given by the LDM as

$$\bar{\mu}_{\mathrm{d}} = \mu_0\left(\coth(X_{\mathrm{d}}) - \frac{1}{X_{\mathrm{d}}}\right)\bar{e} \tag{1}$$

where μ_0 is the total dipole assigned to a lattice site, and $\bar{e}$ is a unit vector that shows the direction of the electric field, $\bar{E}$. The subscript d indicates that the contribution originates from the dipole in the considered lattice site. X_d is defined by

$$X_{\mathrm{d}} = \frac{\mu_0 E}{k_{\mathrm{B}} T} \tag{2}$$

where k_{B} is the Boltzmann constant and T the temperature. The response from the polarizabilities in the lattice sites can be obtained from

$$\bar{\mu}_{\mathrm{e}} = \alpha_{\mathrm{e}}\bar{E} \tag{3}$$

The subscript e indicates that the contribution originates from the electronic degrees of freedom. It must be noted that the electric field and the polarization in the lattice sites are dependent on each other, because the electric field at one lattice point is obtained as the sum of the electric field from the solute and the electric field originating from the total dipoles in the other lattice points. Thus,

$$\bar{E}_{\mathrm{t}} = \bar{E}_0 + \bar{E}_\mu + \bar{E}_{\mathrm{e}} \tag{4}$$

$\bar{E}_0$ is the electric field created by the solute, $\bar{E}_\mu$ is the electric field created by the other Langevin dipoles, and $\bar{E}_{\mathrm{e}}$ represents the field originating from the electronic degrees of freedom in the other lattice sites. Because of this interdependence, the above equations must be solved by an iterative process until self-consistency. Once the solution to these equations is reached and the Langevin dipoles are obtained, the electrostatic contribution to the (free) energy can be calculated.[13,25,26]

The lattice model used in this study has, as indicated above, been slightly modified relative to standard lattice models to remove some of the shortcomings of such models. Furthermore, a dielectric continuum starting outside the used lattice sites has been added to make the method model a system with an infinite environment.

A weakness of the standard implementation of the LDM originates from that the lattice sites and the molecular system to some extent occupying the same part of space. Normally, this is dealt with by saying that, if a lattice site is within a given distance from some atom in the target molecule, then the dipole (and polarizability) of the lattice site is explicitly removed from the calculation. As a consequence, the solvation energy changes discontinuously when the molecule is translated in the lattice. In this work, we have tried an alternative approach, by assuming that there is a repulsive interaction between each atom and each lattice site. In this way, a penalty energy can be calculated for each lattice site. This energy is used to determine how much of the dipole and polarizability should be used in the calculation using a Boltzmann-type expression. This issue will be further discussed in connection with the parametrization of the model in section 3.

As was mentioned, a series of ab initio restricted Hartree−Fock (RHF) close-shelf calculations have been performed on *cis*-UCA using the model outlined above to describe the environmental effects. All calculations in this study have been performed with the MOLCAS package.[27] A small atomic natural orbitals (ANO-S) basis set[28] has been used in the calculations. The carbon, nitrogen, and oxygen basis sets were a (10s6p3d/4s3p2d) contraction. For hydrogen atoms bonded to polar atoms, such as nitrogen and oxygen, a (6s4p/3s2p) contraction was used, while for hydrogen atoms bonded to nonpolar atoms, such as carbon, a (6s4p/3s1p) contraction was employed. Using the conformations obtained in a previous study[5] as starting point, we reoptimized the structures of the neutral, cationic, and anionic *cis*-UCA in gas phase. The calculations using the LDM have been performed employing these gas-phase structures. We believe that the approximations introduced by using these structures will not affect significantly the results and conclusions of this study.

To employ the solvation model as presented above, a set of parameters must be determined. These are the radius of the cavity that embeds the lattice, the size of the lattice, the permanent dipole of each lattice point (μ_0), the polarizability assigned to each lattice point (α), and finally the van der Waals radii of the solute atoms. In the next section, we will discuss the methods used to determine these parameters. The permanent dipole and the polarizability are fixed to get a given value of the relative dielectric permittivity (the dielectric constant). These parameters are obtained by a rearrangement of the Clausius−Mossotti equation:[13]

$$\epsilon = \frac{1 + \frac{8\pi}{3}P}{1 - \frac{4\pi}{3}P} \tag{5}$$

where P, the unit generalized polarizability, is

$$P = \frac{\alpha + \frac{{\mu_0}^2}{3kT}}{V} \tag{6}$$

V is the volume of the lattice cell. Papazyan and Warshel have studied the applicability of the Clausius−Mossotti equation and devised improvements taking the thermal fluctuations into account.[23] A procedure involving several steps has been used to obtain the van der Waals volume of the solute. This is calculated through the van der Waals radius of the atoms that

make up the molecule. In the following section, a detailed explanation of how the radii have been obtained is presented.

3. Parametrization of the Model

The most important parameter in this type of lattice models is the lattice constant (l), that is, the shortest distance between two lattice points. Several different types of aspects could be put on the choice of this parameter. If a very small value is chosen for l, the difference between a Langevin dipole and an ideal polarizability disappears and the model approaches an ordinary dielectric model like PCM. This will also lead to the computation time being very large. On the other hand, if a large value is chosen for l, then packing effects, that is, the position of the target molecule relative to the lattice, will become very important. In this work, we have chosen a lattice constant of 3.0 au as a compromise between the two requirements. This lattice constant should in some way be connected to the bulkiness of the solvent.

The used lattice is embedded in a dielectric medium. The radius of the embedded lattice is 7.75 au, and the dielectric continuum starts at a distance of 8.65 au from the origin. Observe that the outermost lattice sites may not come too close to the dielectric surrounding because this will lead to a divergence in the interaction. The charge distribution on the dielectric boundary is expanded in spherical harmonics, and the expansion is truncated at $l_{max} = 5$.

In a model like the present one, it is necessary to define a partitioning of the space between the solute molecule and the lattice. This is done in the following way. For each lattice site, a penalty energy is defined according to

$$E_{\text{latt}} = \sum^{\text{atoms}} \left(\frac{d_{\text{atom-latt}}}{r_{\text{atom}}} \right)^{10} \tag{7}$$

In this equation, r_{atom} is a radius dependent on atomic type. In this way, we define a penalty energy for each lattice site. The actual lattice site polarizability and dipole moment is obtained from a Boltzmann-type expression:

$$\alpha^i_{\text{latt}} = \alpha^0_{\text{latt}}\, e^{-E_{\text{latt}}/(k_B T)} \tag{8}$$

$$\mu^i_{\text{latt}} = \mu^0_{\text{latt}}\, e^{-E_{\text{latt}}/(k_B T)} \tag{9}$$

If the polarizability and dipole is reduced to less than 1% of the original values, then the lattice point is removed completely from the calculation. The major advantage of the use of eqs 7−9 for modifying the lattice site dipole moments and polarizabilities is that one obtains a much smaller dependence of the position of the molecular system relative to the lattice.

The parametrization of the atomic radii was started by considering the radius for the oxygen and hydrogen atoms. Because the lattice site in some way is meant to represent an atom or molecule in the solvent, we assumed that the size of the hydrogen and the oxygen atoms were the same. This seems natural because the distance from these atoms to their nearest neighbor atoms (at least in water) is the same. To obtain these radii, a self-consistent process was used, a water molecule was considered, and a radius was guessed for these atoms, and then the internal coordinates and the position of the water molecule in the lattice were optimized using a Monte Carlo procedure. The energy of the optimized water molecule in gas phase was subtracted from the optimized energy obtained from condensed-phase calculation. The result is called the solvation energy of the water. The atomic radii were changed, and the optimization was repeated until the solvation energy was −5.5 kcal/mol. This was regarded as a reasonable value for the solvation energy taking into account that the experimental solvation energy for water is about −10 kcal/mol and the contribution of the dispersion term (which is not consider in this model) to this energy is around −4.5 kcal/mol.[29] In this procedure, an optimization was considered converged when the energy difference was lower than 10^{-5} au. Furthermore, the value of μ_0 for the lattice sites was set equal to zero to simplify the calculations. This can be done because the field from the water molecule is so small that hardly any effects of dielectric saturation can be observed. The value of α was 5.155 au, which gives a relative dielectric permittivity of 12.98 according to the Clausius−Mossotti equation. This was the highest value reached before instabilities in the model appear. In fact, this value is somewhat higher than the value of 11.7 at which polarizabilities on a primitive cubic lattice pass a phase transition to an antiferromagnetic phase.[23] This does not occur in our system because of its finite size and the way that the dielectric boundary conditions are implemented.

When the parametrization of the oxygen and hydrogen radii was completed, the radius for the nitrogen atom was determined in a similar way from calculations on the ammonia molecule. The optimized value for this parameter gives a solvation energy of −3.2 kcal/mol for the ammonia molecule. Finally, the radius for the carbon atom was obtained using the cyanide anion. The solvation energy for this molecule was −66.0 kcal/mol. The final values of the radii are 1.63 Å for hydrogen and oxygen, 1.75 Å for nitrogen, and 1.90 Å for carbon.

4. Results

In this work, the LDM have been used to model the effects of the surrounding medium in calculations in which we have studied the relative stability of *cis*-UCA in its different neutral, cationic, and anionic forms. The characterization starts by the optimization of the different conformers in gas phase. The resulting geometries are shown in Figure 1. The final structures are similar to those obtained in a previous work,[5] and there are only minor differences between the two sets of conformers.[30] Once the optimized gas-phase structures were obtained, a calculation for each configuration was performed with the LDM representing human skin. However, we do not know of any measurement of the relative dielectric permittivity of human skin. The way that we have chosen to handle this situation is to test several values for the relative dielectric permittivity. It was assumed that the relative dielectric permittivity at high frequencies (due to the electronic degrees of freedom) must be around 2, a value observed for most liquids and solids of organic origin (the corresponding value for water is 1.8). Using eqs 5 and 6, we computed a polarizability of 1.357 au, which corresponds to a high-frequency relative dielectric permittivity of 1.8 (the value obtained for water). If we again use these equations together with the established polarizability, we obtain a magnitude of the dipole of 0.0276, 0.0606, 0.0835, and 0.0973 au for a total relative dielectric permittivity of 2.0, 3.0, 5.0, and 8.0, respectively. The obtained relative energies for the different conformations in gas phase using the LDM are tabulated in Table 1. The radius of the embedded lattice is 12.7 au, and the dielectric continuum starts at 13.5 au, the remaining parameters of LDM were kept at the same values as those used in the parametrization of the model. It can be seen that in gas phase the neutral conformer with an IMHB between the oxygen and the hydrogen (conformer **A**) is 6.95 kcal/mol more stable than the conformer with the IMHB between the nitrogen and the

TABLE 1: Relative Energies (kcal/mol) for the Neutral (A, B), Cationic (C), and Anionic (D, E) *cis*-UCA Molecule in Gas Phase and with the Langevin Dipole Model[a]

	species				
	A	**B**	**C**[b]	**D**	**E**
gas phase	239.99	246.94	0.00	584.65	586.63
solvated[c]	274.76	275.74	0.00	585.09	582.89

[a] Geometries optimized in gas phase. [b] Absolute energies are −489.856 39 and −489.919 84 au in gas phase and solvated, respectively. [c] LDM with a relative dielectric permittivity of 5.

TABLE 2: Dipole Moments (au) for the Neutral (A, B), Cationic (C), and Anionic (D, E) *cis*-UCA Molecule in Gas Phase with the Langevin Dipole Model

	species				
	A	**B**	**C**	**D**	**E**
gas phase	1.046	4.228	2.798	1.009	2.394
solvated	1.276	5.094	3.240	1.245	2.928

hydrogen (conformer **B**). The opposite behavior is found for the anionic forms (**D** and **E**) for which the conformer with the IMHB between the nitrogen and the hydrogen is 1.98 kcal/mol more stable. When the effect of the surrounding medium is included, using a relative dielectric permittivity of 5.0, the energy difference decreases to 0.98 kcal/mol for the neutral conformations and the relative stability changes between the two the anionic forms, with the **E** configuration being 2.2 kcal/mol more stable than the **D** conformer in the medium. The difference in solvation energy for the neutral structures and the anionic forms are 5.97 and 4.18 kcal/mol, respectively. In Table 2, the dipoles of the different conformations are given in gas phase and with the LDM model. This table shows that the conformers that gain stability have a bigger dipole moment than the others. Thus, the dipole moment of the **B** conformer is bigger than that of **A**, and the same happens between **E** and **D**. The relative increase of the dipole moments from gas phase to condensed phase is between 16% and 23%.

Once the energies for the different conformations was obtained, we focused on the reaction barrier between the two anionic forms and how it changes from gas to condensed phase. In a first attempt to study this, we calculated the energy barrier of the isomerization process between the **D** and **E** conformers in gas phase. As a first approximation, the energy profile was studied as a function of a linear interpolation between the structures of the **D** and **E** species (see Figure 2). It can be seen that there is an energy barrier around 10 kcal/mol with respect to the **D** structure and around 12.5 kcal/mol if the **E** conformer is used as reference. The used procedure is likely to yield an energy barrier that is too high.

To obtain a more reliable result, the transition state in gas phase was first located. When the transition state in gas phase was found, a point calculation with the LDM for that geometry was done. The energies of the transition state between **D** and **E** in gas phase and the corresponding values obtained using the LDM are given in Table 3 for different values of the relative dielectric permittivity. The energies for the **D** and **E** forms are also shown. The transition state obtained in this way is significantly lower than the one calculated earlier by an interpolation procedure between **D** and **E**. The new energy barrier between the **E** and **D** forms is 6.2 kcal/mol compared to the old one, which was 12.5 kcal/mol. To obtain an energy profile for the reaction, a similar procedure as was followed before was used to obtain Figure 3. However, this was done in two steps. The first half of the geometries studied in the calculations was obtained by interpolating between the **D** conformer and the transition state. The other half was constructed using an interpolation between the transition state and the **E** configuration. Figure 3 shows the new reaction path obtained by this two-step procedure. We can see that the transition state is the configuration with highest energy and that the points closest to the assumed transition state are more stable. This seems to indicate that the used gas-phase optimized geometries in connection with the LDM are not a bad approximation and that the real transition state for the proton-transfer reaction in the *cis*-UCA in a medium can be described as done here.

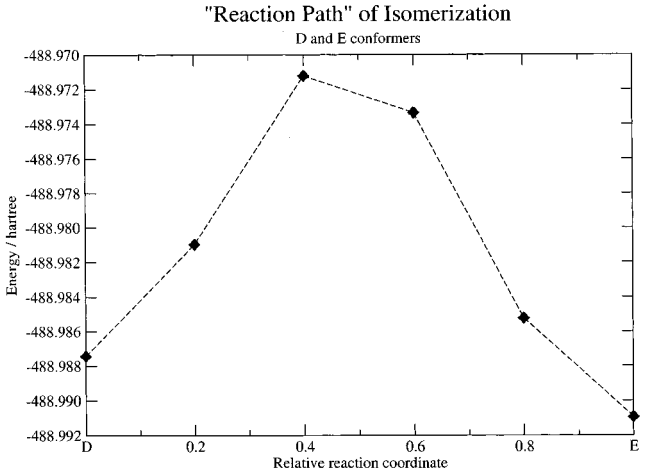

Figure 2. "Reaction path" of the isomerization between the **D** and **E** conformers using **D** and **E** as reference points in the interpolation procedure (see text for details).

TABLE 3: The Relative Energies (kcal/mol) for the Anionic (D, E) *cis*-UCA Structures and the Corresponding Transition State (TS) as a Function of the Relative Dielectric Permittivity[a]

	relative dielectric permittivity				
structure	1.0[b]	2.0	3.0	5.0	8.0
D	−1.98	0.26	1.26	2.20	2.83
TS	4.06	5.26	5.74	6.16	6.41
E	0.00[c]	0.00[d]	0.00[e]	0.00[f]	0.00[g]

[a] Geometries optimized in gas phase. [b] In gas phase. [c] Absolute energy −488.921 54 au. [d] Absolute energy −488.962 49 au. [e] Absolute energy −488.977 75 au. [f] Absolute energy −488.990 94 au. [g] Absolute energy −488.999 00 au.

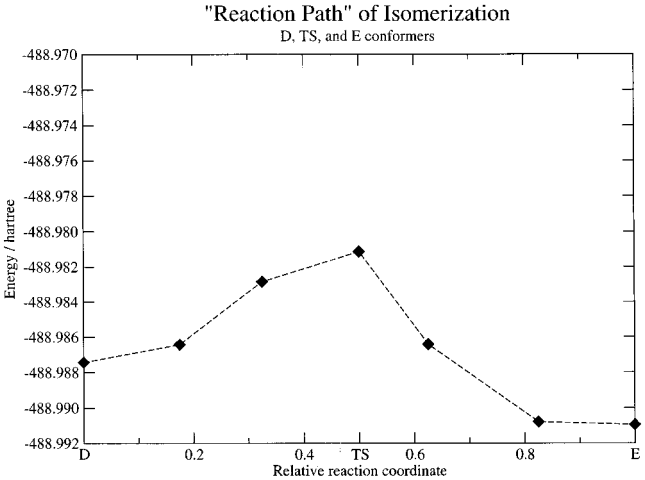

Figure 3. "Reaction path" of the isomerization between the **D** and **E** conformers using **D**, **E**, and the transition state (**TS**) as reference points in the interpolation procedure (see text for details).

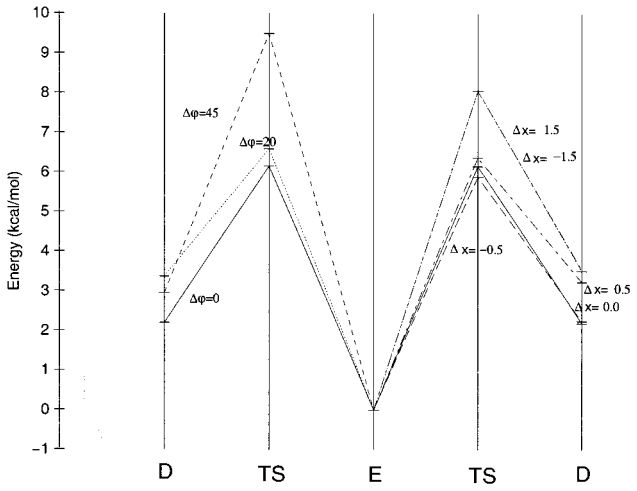

Figure 4. Energy barriers (kcal/mol) of the **D** and **E** *cis*-UCA conformations and the (**TS**) obtained by translation (au) along one of the axes in the molecular plane and by rotation (deg) around the axis perpendicular to the molecular plane.

The results of this study will depend to some extent on the position and orientation of the molecule relative to the lattice. To obtain a measure of this, we have studied the variation of the system energy as a function of the position and orientation of **D**, **E**, and **TS**. In the right half of Figure 4, we present the variations in the obtained relative stabilities for the **D**, **E**, and **TS** forms obtained when the molecular system is translated −1.5, −0.5, 0.0, 0.5, and 1.5 au relative to the lattice. A similar procedure has been followed to study the effect of rotating the molecules around an axis perpendicular to the molecular plane instead of translating them. In the left half of Figure 4, we present the influence of rotation on the reaction energetics. For the translations, the highest barriers occur for translations of 1.5 and −1.5 au with respect to the original origin (those points are almost equals because of the symmetry of the cell). The highest barrier is observed when the molecules are rotated 45°. The obtained barrier is around 9.5 kcal/mol. This last barrier is produced for a very unfavorable position of the **TS** conformation in the cell. The most accurate way to obtain the barrier will require the optimization of the position of each conformation, **D**, **E**, and **TS**, in the cell and the calculation of the energy for each of these optimized structures. The improvement of the result will be small, and if we take into account the uncertainty of the method and that the cost of it will be very high, it is most likely not worth the effort. With use of the calculations already performed and taking the most favorable point for each conformer, the barrier between **E** and **TS** will raise by 1.70 kcal/mol with respect to the original value. We have also calculated the barrier using the polarizable continuum model (PCM).[31,32] It is found to be 10.96 kcal/mol from **E** to the **TS**, and the energy difference between **D** and **E** is 4.39 kcal/mol. Those calculations have been done using the defaults parameters in MOLCAS 5.2 for water as solvent, and the dielectric permittivity was set to 5.0. The results of the PCM correspond to a higher barrier than the LDM, but that could change if the size of the cavity is changed. This cavity size in the PCM model is to certain extend an analogous parameter to the position of the molecule in the cell for the LDM model.

A weak point in this modeling is that the relative dielectric permittivity of the skin is unknown. Calculations have been done to study the influence of the relative dielectric permittivity on the relative stability of the **D** and **E** conformers and the transition state. Point calculations with the LDM were performed using values of 2, 3, 5, and 8 for the relative dielectric permittivity of the surrounding medium. The resulting energies from these calculations together with the energies for gas phase are given in Table 3. From the results, it can be deduced that with an increasing relative dielectric permittivity follows a corresponding stabilization of **E** as compared to the two other anionic structures. The explanation is simple. When the negative charge is located at the CO_2 part of the molecule, it is confined to a smaller volume than when it is located at the imidazol ring. The solvation energy for a localized charge is larger than that for a delocalized charge.

5. Conclusions

In this work, we have presented a modified quantum chemical Langevin dipole model in which *both dipoles and polarizabilities* have been placed on the lattice sites of a primitive cubic lattice. The modified model uses a penalty function to model the repulsion of the atoms of the quantum system on the lattice points. This repulsive interaction is allowed to modify the lattice site polarizability using a Boltzmann-type expression. Furthermore, a dielectric continuum is added to pick up contributions from outside the range of the finite lattice.

The model has been used to study different forms of *cis*-UCA in a condensed phase with values of the relative dielectric permittivity ranging from 2 to 8. The different values have been chosen because the dielectric properties present in human skin are unknown but could be expected to fall within the studied range. The dielectric medium calculations exhibit a stabilization of the less-stable configurations in gas phase, in which the charge is located at the carboxylic group, relative to the more-stable conformations in gas phase, in which the charge is located at the imidazole ring. The solvent effects change the relative stability of the anionic species. The characterization of the transition state of the proton-transfer reaction occurring in the anionic forms of *cis*-UCA predicts that the reaction energy barrier with respect to the **E** conformation increases when the relative dielectric permittivity increases. The observed effect can be understood from the fact that a larger solvation energy can be expected from structures in which the negative charge is located at the smaller carboxylic group rather than at the larger imidazole ring. The calculations also indicate that the energy of the two anionic forms is almost the same under the conditions present in vivo. This may naturally be a coincidence, but it may also be linked to the biological functioning of the compound. In particular, we note that the polarizability of the system will be very large if the nuclear contribution to the polarizability is included. This may be biologically significant.

Acknowledgment. J.M.H.-R. thanks the "Ministerio de Educación, Cultura y Deporte" for award of research grant.

References and Notes

(1) Quinn, R.; Mercer-Smith, J.; Burstyn, J. N.; Valentine, J. S. *J. Am. Chem. Soc.* **1984**, *106*, 4136.

(2) Mawlawi, H.; Monje, M. C.; Lattes, A.; Rivière, J. *J. Heterocycl. Chem.* **1992**, *29*, 1621.

(3) Roberts, J. R.; Yu, C.; Flanagan, C.; Birdseye, T. R. *J. Am. Chem. Soc.* **1982**, *104*, 3945.

(4) Lathi, A.; Hotokka, M.; Neuvonen, K.; Äyräs, P. J. *J. Mol. Struct. (THEOCHEM)* **1995**, *331*, 169.

(5) Lathi, A.; Hotokka, M.; Neuvonen, K.; Karlström, G. *J. Mol. Struct. (THEOCHEM)* **1998**, *452*, 185.

(6) De Fabo, E.; Noonan, F. J. *Exp. Med.* **1983**, *157*, 84.

(7) Morrison, H. *Photodermatology* **1985**, *2*, 158.

(8) Norval, M.; Simpson, T. J.; Ross, J. A. *Photochem. Photobiol.* **1989**, *50*, 267.

(9) Norval, M.; Gibbs, N. K.; Gilmour, J. *Photochem. Photobiol.* **1995**, *62*, 209.
(10) Bertolasi, V.; Nanni, L.; Gilli, P.; Ferretti, V.; Gilli, G.; Issa, Y. M.; Sherif, O. E. *New J. Chem.* **1994**, *18*, 251.
(11) Zimmerman, S. C.; Korthals, J. S.; Cramer, K. D. *Tetrahedron* **1991**, *47*, 2649.
(12) Frey, P. A.; Whitt, S. A.; Tobin, J. B. *Science* **1994**, *264*, 1927.
(13) Böttcher, C. J. F.; van Belle, O. C.; Bordewijk, P.; Rip, A. *Theory of Electric Polarization*; Elsevier: Amsterdam, 1973; Vol. 1.
(14) Orozco, M.; Luque, F. J. *Chem. Rev.* **2000**, *100*, 4187.
(15) Warshel, A.; Åqvist, J. *Annu. Rev. Biophys. Biophys. Chem.* **1991**, *20*, 267.
(16) Warshel, A. *Computer Modeling of Chemical Reactions in Enzymes and Solutions*; Wiley: New York, 1991.
(17) Warshel, A.; Levitt, M. *J. Mol. Biol.* **1976**, *103*, 227.
(18) Warshel, A. *J. Phys. Chem.* **1979**, *83*, 1640.
(19) Heller, H.; Grubmüller, H.; Achulten, K. *Mol. Simul.* **1990**, *5*, 133.
(20) Tanford, C.; Roxby, R. *Biochemistry* **1972**, *11*, 2192.
(21) Florian, J.; Warshel, A. *J. Phys. Chem. B* **1999**, *103*, 10282.
(22) van Belle, D.; Couplet, I.; Prevost, M.; Wodak, S. J. *J. Mol. Biol.* **1987**, *198*, 721.
(23) Papazyan, A.; Warshel, A. *J. Phys. Chem. B* **1997**, *101*, 11254.
(24) Luzhkov, V.; Warshel, A. *J. Am. Chem. Soc.* **1991**, *113*, 4491.
(25) Warshel, A.; Russel, S. T. *Q. Rev. Biophys.* **1984**, *17*, 283.
(26) King, G.; Warshel, A. *J. Chem. Phys.* **1989**, *91*, 3647.
(27) Andersson, K.; Baryz, M.; Bernhardsson, A.; Blomberg, M. R. A.; Boussard, P.; Cooper, D. L.; Fleig, T.; Fülscher, M. P.; Hess, B.; Karlström, G.; Lindh, R.; Malmqvist, P.; Neogrady, P.; Olsen, J.; Roos, B. O.; Sadlej, A. J.; Schimmelpfennig, B.; Schütz, M.; Seijo, L.; Serrano, L.; Siegbahn, P. E.; Stålring, J.; Thorsteinsson, T.; Veryazov, V.; Wahlgren, U.; Widmark, P. *MOLCAS*, version 5.0; Department of Theoretical Chemistry, Chemical Center, University of Lund: Lund, Sweden, 2000.
(28) Widmark, P. O.; Malmqvist, P.-A.; Roos, B. O. *Theor. Chim. Acta* **1990**, *77*, 291.
(29) Åstrand, P.-O. Hydrogen Bonding as Described by Perturbation Theory. Ph.D. Thesis, Theoretical Chemistry, Chemical Center, University of Lund, Lund, Sweden, 1994.
(30) The molecular coordinates for these gas-phase geometries will be provided on request to the authors.
(31) Miertus, S.; Scrocco, E.; Tomasi, J. *Chem. Phys.* **1981**, *55*, 117.
(32) Miertus, S.; Tomasi, J. *Chem. Phys.* **1982**, *65*, 239.